Hindawi Publishing Corporation
Journal of Robotics
Volume 2012, Article ID 826364, 16 pages
doi:10.1155/2012/826364

Research Article

Mechanical Description of a Hyper-Redundant Robot Joint Mechanism Used for a Design of a Biomimetic Robotic Fish

M. O. Afolayan, D. S. Yawas, C. O. Folayan, and S. Y. Aku

Mechanical Engineering Department, Ahmadu Bello University, Samaru, Kaduna, P.O. Box 504, Zaria, Nigeria

Correspondence should be addressed to M. O. Afolayan, tunde_afolayan@yahoo.com

Received 24 October 2011; Revised 5 January 2012; Accepted 30 January 2012

Academic Editor: Shugen Ma

A biologically inspired robot in the form of fish (mackerel) model using rubber (as the biomimetic material) for its hyper-redundant joint is presented in this paper. Computerized simulation of the most critical part of the model (the peduncle) shows that the rubber joints will be able to take up the stress that will be created. Furthermore, the frequency-induced softening of the rubber used was found to be critical if the joints are going to oscillate at frequency above 25 Hz. The robotic fish was able to attain a speed of 0.985 m/s while the tail beats at a maximum of 1.7 Hz when tested inside water. Furthermore, a minimum turning radius of 0.8 m (approximately 2 times the fish body length) was achieved.

1. Robotic Trends

According to Peters [1], biomimetic robots, and evolutionary robots, emotion-controlled robots are ideas imitating life not with different approaches but with a common goal of improving the adaptivity and learning capabilities of robots, thus "breeding" a new generation of robots with better "survival" chances in their specific operational environment. Several functional biologically inspired robots are already in service [2] such as Sony AIBO, Honda ASIMO, Toyota Flute playing robot, Wall gecko (wall climbing robot) from Stanford University, and lately DARPA humming bird robot. Biomimetic robots imitate some characteristics of life forms such as mobility [3], vision [3–7], flying [3, 7, 8], and navigational methodology. Biomimetic systems are greatly desired because natural systems are highly optimized and efficient. Srinivasan [6] calls them shortcuts to mathematically complex issues of life. Take a look at fly or honey bee, they have very small brain and processing power, no researcher has ever built a robot with such visual capabilities like them at such a scale at least to our knowledge. Nearly all the five senses of living beings, that is, sight or vision [3, 7], hearing and touch (http://world.honda.com/ASIMO/ and http://www.sony.net/Products/aibo/index.html), smell [9], and taste (http://www.21stcentury.co.uk/robotics/nomad.asp) are imitated. The semiautonomous indoor airplane by [3] was only possible because of its mimicry of insect vision using optical flow.

2. Hyper-Redundant Robots

These are robots in the form of serpentine or snake or rod shape. Snakes, tentacle, trunk, and fish are examples of biological hyper-redundant bodies. The redundancy means different ways to perform the same movement and is usually denoted in terms of degrees of freedom.

Robots with a snake-like locomotion have these *advantages:*

(1) the redundancy allows them to still function after losing mobility in one or more sections;

(2) stability on all terrain because of low center of gravity;

(3) terrainability which is the ability to traverse rough terrain;

(4) traction is very high as the whole body is involved;

(5) high efficiency in energy use as there is no need to lift the body;

(6) small size that can penetrate small crevices;

(7) they are capable of being amphibious by sealing the whole body, the same body motion on land is then

Worm

Snake

Millipede

Elephant trunk

Fish

Figure 1: Examples of biological hyper-redundant bodies. Source [14].

used for swimming in water as exemplified by ACM-R5 robot [10, 11].

The *disadvantages* include:

(1) low speed as the whole body is used for motion, [12];

(2) poor thermal control because of low surface to volume ratio, [13];

(3) how to control, programme, and build an efficient control system for the several degrees of freedom (DOF) links or joints.

3. Examples of Biological Hyper-Redundant Bodies

Figure 1 shows some examples of biological hyper-redundant bodies. The worm, millipede, and elephant trunk have no bone while the fish and snake have bony support.

4. Scenario Requiring Hyper-Redundant Robot

Examples of scenario requiring hyper-redundant robots are:

(i) under water devices (like submarine cables) requiring automated inspections;

(ii) searching and rescuing among rubble such as in collapsed building;

(iii) cheap and distributed space exploration robots—[15];

(iv) firefighting (acting like intelligent fire hose that can autonomously locate fire);

(v) manufacturing and machine maintenance in a convoluted environment [16];

(vi) general manufacturing, they can act as robotic arm with great dexterity;

(vii) minimally invasive surgery, as laparoscope or endoscope that can follow a very complex path without colliding or penetrating organs;

(viii) stealth perimeter surveillance especially if the model is mobile, for example snake form for residential areas, fish form for antiscuba in lagoons and estuaries. If made smaller, that is, as autonomous microrobots, it can be used for security checkups in difficult scenarios for example, hostage, enemy camps, collapsed structures, pipe inspection, and so forth, where human presence is not desirable.

5. Statement of the Problem

The standard problems normally encountered in hyper-redundant robot designs are:

(1) how to control the multiple degree of freedom joints to produce usable motion [13, 17–23]. A hyper-redundant body can take a very large number of possible shapes without a constraint;

(2) the effective actuator design that will have enough strength and tenacity to carry the weight of other

links [24], powerful and fast enough while not generating too much heat [23];

(3) how better biomimicry can be done in designing a hyper-redundant joint. Biological systems, for example, hydrostatic skeletons, are commonly found in the form of invertebrate as a complete organism and as part of an organ (such s tongue) in the case of vertebrates. Invertebrates have *almost* a continuum body while vertebrate such as snakes have over 200 vertebras (200-1 joints) to support their bodies. An elephant trunk has no single joint, that is, it is continuum;

(4) how can the complex control strategy be simplified like that of the biological systems. Most researchers have been extrapolating convectional joints-hinge, universal, even ball and sockets in an attempt to build hyper-redundant robot. These approaches have made many of those robots unsuccessful in their imitation of nature. Octopus has no bone in its tentacles but it is able to control its motion so effectively as to attract researchers [25–27]. The simplicity of the control strategy it used was referred to as being stereotypical and is worthy of imitating.

6. The Objective of This paper

The main objective of this paper is translating a biological model (Mackerel) into a robotic model. Furthermore, we aimed at

(1) implementing the design using lessons from nature hydrostatic skeleton designs;

(2) designing the hyper-redundant robot joint using materials closest to biological tissues;

(3) assessing the possibility of using carbon filled rubber as the biomimetic material.

These goals are justified because translating a biological model into a robotic model could follow myriad of possible ways as reviewed in this paper with some leading to imitation only in shape but weak or too strong mechanically.

7. Review of Past Work

The term hyper-redundant robot was introduced by Chirikjian and Burdick [28] in the early 1990 to describe robots with numerous independent degrees of freedom (DOF). Hyper-redundant robot falls into two broad categories:

(1) mobile hyper-redundant robots such as snake robots and serpentine robots: the snake robots are multisegment mechanism that derives propulsion from the relative motion of the joints only. They use no wheels, legs, or tracks for propulsion. Examples are Gavin Miller S1 to S7 Snake robots [29]. The serpentine robots are multisegment mechanism that derives propulsion from wheels, legs or tracks. Joints connecting the segments may be powered. Examples are KR-I [30], MOIRA [31], OmniTread, and OmniPede [32];

(2) fixed base robots: these are a subclass of snake robots that have one of their ends fixed. An example is the Urban Search and Rescue Elephant Trunk Robot (USAR ETR) from Carnegie Mellon University (http://www.snakerobot.com/).

7.1. Robotic Joints Designs. The *convectional robots* can best be described as discrete manipulators [24], where the designs are based on a small number of actuatable joints that are serially connected by discrete rigid link. The *Hyper-redundant robots* on the other hand have larger number of joints while *Continuum robots* theoretically have no joints or the joints are not distinct.

7.2. Hyper-Redundant Robot Joint Implementations. According to [33], most researchers build their biologically inspired hyper-redundant robots from concatenated rigid modules with multiaxis joints [34], universal joint [35, 36] or revolute joint [37], parallel mechanism [17], and some are hybrid [18]. Similar modular designs have been used as reconformable machines [19] and form the basis for many undulating or swimming robots [20, 21]. Examples of hyper-redundant robot joint implementations are:

(1) revolute joint [37];

(2) universal joint [11, 16]. It is the most popular joint adopted;

(3) parallel mechanism [17];

(4) angular swivel joint with Universal Joint [38];

(5) angular swivel joint with bevel gear train joint [39].

Joints based on oblique mechanism are used for slowly changing joint angle such as used by MOGURA for manufacturing and Carnegie Mellon University elephant trunk robot.

7.3. Joint Types Found in Biological Models. The biological models are hereby grouped as *vertebrate* and *invertebrate*. For the vertebrates, we have ball and socket, ellipsoid joint, pivot joint, hinge or revolute joint, saddle joint, plane joint, boneless joints (*muscular hydrostats*) like in trunk (elephant and opossum), tentacles (octopus and squid), tongue, mammalian penis, and cochlea (hearing frequency filter).

Most invertebrate organisms have very simple body structure, mostly tubular. Their bodies are supported by water or their fluidic habitat [40]. For the larger ones, two methods of supports were evolved; one method uses fluid-filled balloon-like elastic structure for support [40–42]. The fluid includes blood, intracellular fluid, and seawater depending on the animal *Taxa*. The incompressibility of these water based fluid and a flexible restraints/container act as the skeleton—hence hydrostatic skeleton.

7.4. Hydrostatic Skeletons. There are 2 types of hydrostatic skeletons, the *first* type, referred to as *muscular hydrostats,* have muscle and other tissues forming a solid structure

Figure 2: A lateral view of a Mackerel. This sample (394.01 mm long) was translated into CAD model and the robot construction was based on it.

without a separate enclosed fluid volume for example, cephalopod tentacles, elephant trunks, and vertebrate tongue [22, 26, 27]. In the *second* type, muscle composed a body wall like balloon and surrounds a fluid-filled space, for example, sea anemones and worms [40]. According to [22, 25–27], a muscular hydrostat consists of closely packed arrays of muscle fibers organized in 3 main directions—parallel, perpendicular, and helical or oblique to the long axis. According to Kier and Smith [22], there are 4 elementary movements that a hydrostat body can make; elongation, shortening, torsion, and bending at any point in its length.

Hydrostatic are of two forms in terms of volume:

(i) sectional isochoric (constant volume sections) as exemplified by Leech—*Hirudo medicinalis* [23];

(ii) whole-body isochoric (constant volume of the whole body) for example, Tobacco hornworm caterpillar—(*Manduca sexta*), [43].

7.5. Biological Materials Stress-Strain Nature. Biological materials stress-strain relationship has been shown to be *hyper-elastic* in nature—[44]. The stress-strain behaviour is qualitatively the same with non biological materials, especially black carbon filled rubber. For example Fung-elastic exponential model have been used to model elastin [45] while *manduca sexta* muscles was modeled by using Ogden and Roxburgh hyper elastic model [44, 46]. The implication of these is that black carbon filled rubber can be used as building material for true biomimicry.

7.6. Some Examples of Hyper-Redundant Robot. Active cord mechanism (ACM) is the first serpentine robot built by Shiego Hirose in 1970 at the Tokyo Institute of Technology. ACM III and ACM R2 (Revision 2) were both planar. That is, each segment can only move in a plane relative to the other (1 degree of freedom). ACM-R3 and ACM-R5 have two degree of freedom joints and ACM-R5 is amphibious with replaceable joints (auto configured) in case of failures. All the ACM have passive wheels except ACM-R3 that uses active wheels for locomotion. ACM-R5 uses 32 bit microcontroller also.

Another hyper-redundant robot described in [47] was named GMD. It uses a flexible compression joint actuated by winding and unwinding a wire about a motorized shaft. The shaft was placed in the middle of the joint. This approach enhanced the biological accuracy. It increased the smoothness of the body and decreased the discontinuities in motion shapes.

Carnegie Mellon University Elephant Trunk Robot was a response to development of Urban Search and Rescue Robot (USAR). An Elephant trunk robot (ETR) based on a new (patented) joint design called angular bevel was described in [39, 48]. Part of the goal was that the joint should be strong enough to lift up rubbles on top victims of a disaster.

Germany sewer and pipe inspection robot MAKRO (multi-segment robot, operating autonomously in sewer pipes) [49] could navigation autonomously in sewer pipes by using several sensors on both ends—laser cross-air, 2-infrared sensor, ultrasonic sensor and transmitter, and a camera, it also has oblique joints.

Pneu-Worm Robot or Wormbot is a commercial robot and much is not disclosed about its operation, it is used for pipe inspection [50]. It uses twin bellow and inchworm motion method for moving within the pipe. The robot is tethered (power and airline supplies the bellows). It carries a camera on its front end and a remote monitor is supplied with it.

NASA Snakebot—for space exploration—is based on Mark Yim Polybot, [51]. It could have countless reconfigurations and accidental loss of a segment will not affect the other—in fact, they will be able to function independently as each segment has its own microcontroller. NASA robot will carry touch sensor over its body. They are expected to help with Martian landscape exploration as they dig into soil, burrow down to depths that other robotic probes cannot get into, slither into cracks, and navigate rough terrain where wheeled and legged robots will get stuck or topple. Since they will be more durable and cheaper, large number can be sent to explore MARS.

MOGURA (a manufacturing arm) was developed between 1982–1984 by Hirose and Yoneda Robotics Lab (Japan) [52] for grinding the water runner of the water wheel for hydroelectric power generation. MOGURA arm uses an oblique swivel mechanism. OBLIX is a variation that has wheels attached.

OmniTread is an example of serpentine robot [53]: OmniTread 8″ is pneumatically driven externally with dual rubber tracks per side (i.e., 8 per segment). The OmniTread 4″ carries its own air supply onboard and has one track per side (or 4 tracks per segment). Both have bellow joint for turning.

7.7. Some Examples of Robotic Fish. Fish are known for their fulgurating acceleration inside water. It is well known that the tuna swims with high speed and high efficiency, the pike accelerates in a flash and the eel swims skillfully into narrow holes. Such astonishing swimming ability inspires several researchers [54–60] to improve the performance of aquatic man-made systems. Unlike conventional rotary propeller used in ship or underwater vehicles, the undulating movement of the fish body is used for its propulsion. The observation on the real fish shows that this kind of propulsion is almost noiseless, effective, and more maneuverable than the propeller-based motions [61].

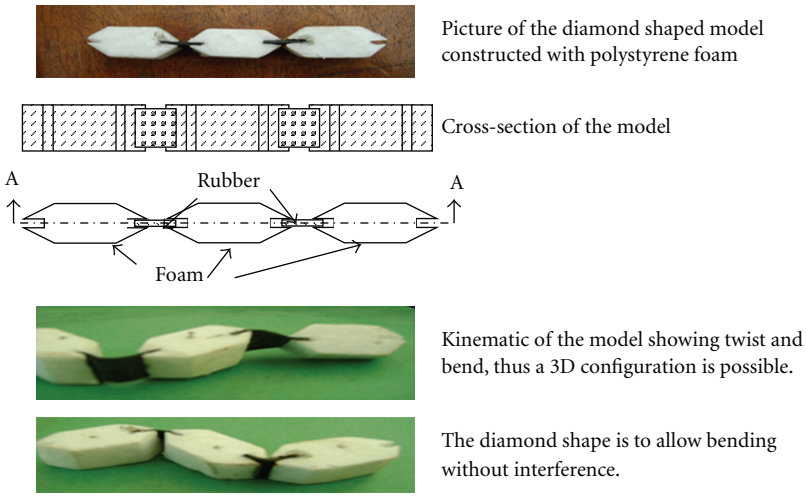

Figure 3: Translation of rubber into artificial hydrostatic joint.

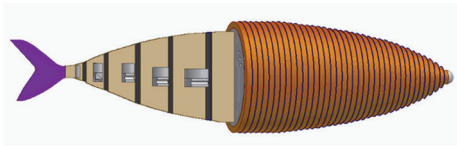

Figure 4: The CAD model of the fish robot. The front part (approximately half) is a rigid haul and the rest part (the tail) is flexible joint of rubber and wooden support.

Four robotic fish models are reviewed in this work; they are Robotuna, Robopike, PF series, and University of Essex fish robot.

Robotuna was developed at Massachusetts Institute of Technology, USA [62]. It uses delrin plastic for most of its construction and epoxy for sealing. It could not float because of the weight and other heavy material used for its construction (3.6 kg). It uses Onset model 8 computer (68332) with digital wireless modem for communication. The tail is made up of rings of delrin plastic.

Robopike is also from Massachusetts Institute of Technology, USA [63]. It was a continuation of work on Robotuna. The pike (a fish) was chosen because of its excellent accelerating and turning abilities. Pike has very quick turning and fast acceleration from a stop. In the wild, pike accelerates at rates to 8–12 m/s^2. Robopike uses only three segments, thus the size of the fish is reduced, allowing the use of inexpensive actuators. This means that while the shape of the fish cannot be made to resemble exactly the shape of a real fish, but a close shape can be obtained. The robot is controlled by a supervisory controller. The navigation is performed by human, and a computer interprets the controls so that the robot can perform as expected. The tail is made up of spiral spring exoskeleton using delrin.

Japanese PF-300, PF-600, PF-700, UPF-2001 robotic fishes were designed for different purposes. The *PF-300* is for studying turning performance and straight forward propulsion. The *PF-600* is designed to study propulsion. *PF-700* is designed for high speed; it has a D/C motor as a power source. The shape was modeled after mackerel and pike, so the PF-700 has very slim body. *PF-2001* is designed to exploit 3D motion. It has the up-down motion mechanism with a moving weight—[64].

Essex G9 robotic fish is about 52 cm long and has 3 powerful R/C servo motors and 2 DC motors. Three servomotors are concatenated together (for the G9 but more than that for other series developed) in the tail to act as 3 joints, 1 DC motors are fixed in the head to change center of gravity of the fish and 1 DC motor controls the micropump. On the back of the fish body, a dorsal fin is fixed vertically to keep fish from swaging. The soft structure of the tail makes it possible for the robotic fish to bend its body at a big angle in a short time (about 90°/0.20 sec). The central controller of the robotic fish is based on a 400 MHz Gumstix Linux computer and is responsible for sampling data from sensors, processing data, making decisions [60, 61].

8. Material

8.1. Materials Selection. The following materials was used in constructing the rubber joints and assembling the robot:

(1) vulcanized rubber—1.5 mm thick;
(2) 1/8 inch (3.175 mm) thick seasoned plywood;
(3) 3/4 (19.05 mm) inch plywood;
(4) four minutes setting Epoxy glue—araldite;
(5) nylon 1010 cables—0.5 mm diameter;
(6) 2.5 mm diameter polythene tubes;
(7) remote control servomotors (Futaba 3003);
(8) microcontroller—PIC18F4520;
(9) a live mackerel (394.01 mm).

The *rubber* is carbon-filled and vulcanized motor car inner tube (14 inch or 35.56 cm) from King Rubber Tire Company of China. It was used for the artificial hydrostatic joint.

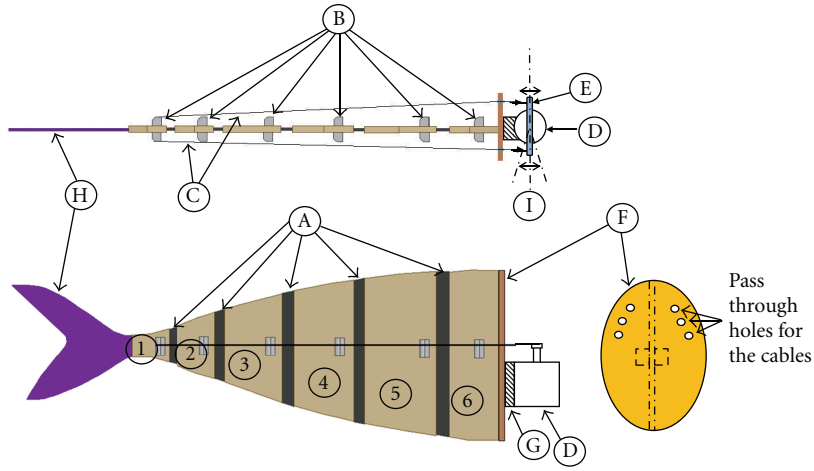

Figure 5: CAD model of the hydrostatic joints (of the tail) showing cables connected to the first segment only.

The *1/8 inch (3.175 mm) thick seasoned plywood* act as support for the rubber material, this is equivalent to insect cuticle. The open air seasoning is for dimensional stability. The *3/4 inch (19.05 mm) plywood* was used for the pulleys. *Epoxy glue* was used for assembly of the parts. The 0.5 mm *nylon cables* connect the servomotor horn (lever) to the joints. The *2.5 mm unplasticized PVC tubing* was used for supporting the nylon cables. The remote control *servomotors* (Futaba 3003) are the programmable actuators (like muscle) that respond to the *microcontroller* instructions.

Biological hyper-redundant bodies vary in length, some are longer like the snake and some are relatively short—like the fish and caterpillars. The control system grows in complexity with their length; many actuators (muscles) will have to be managed simultaneously. A shorter model is used in this work. The high speed teleost species of fish was therefore selected. Examples of teleost fish are mackerel, tuna, and salmon. The specie of teleost fish selected was Mackerel (Figure 2) because of the following reasons:

(1) it is very common;

(2) it is capable of fair speed, 11 km/h;

(3) it is small enough for monitoring shallow water as well as for ecological study.

9. Methodology

9.1. The Artificial Hydrostatic Joint Concept. The design used in this paper is basically an artificial hydrostatic joint. Rubber is used to form the revolute joints because of its closeness to biological material. The joints are basically concatenated diamond shaped structure (or support) interconnected with rubber stripes as shown in Figure 3. The diamond shape is to allow bending without interference.

9.2. The Description of the Rubber Joint Mechanism. Figure 4 shows the CAD model of the robot. The active part of the model that is, the tails is hereby described, the front part is a rigid haul. Using the sketch models shown in Figures 5–7, the manner the joint works is described as follows:

(1) the rubber joint (A) (a stripe of rubber) is sandwiched between pairs of rigid support segments (1) to (6). The tail fin (H) is rigidly connected to the segment (1);

(2) on both sides of each segment (1) to (6) are located a quarter pulleys (B) over which the nylon cable (C) passes before hooking it to those segments;

(3) the nylon cables (C) are attached to the servomotor horn (E);

(4) the servomotor (E) is attached to an oval support (F) having pass through holes for the cables (C) using a glue (G);

(5) the microcontroller sends the angular displacement information to the servomotors (D) in such a manner that its horn (E) will oscillate ± angle (I);

(6) to get a serpentine motion, the microcontroller uses its built in pattern generator to control the sequence of segment ((1) to (6)) turning by activating the servomotor (E)—one is shown for clarity according to the pattern;

(7) the segments (1), (3), and (5) are connected to a servomotor each;

(8) the other segment simplifies the design as they act to restore the joints to its static state. Also, they help in getting the desired serpentine shape without complicated design—just like nature has being simplifying its designs by appropriate use of material. Furthermore this approach simplifies the number of motor required and hence the control scheme,

(9) Figure 6 shows how the tail fin will bend to the left or right when the left or right cable is pulled, respectively by the servomotor (E);

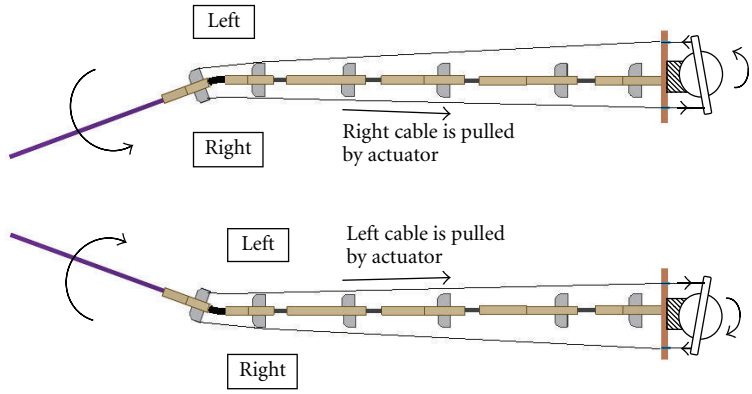

Figure 6: How the tail fin will respond as the actuator pull on the cables.

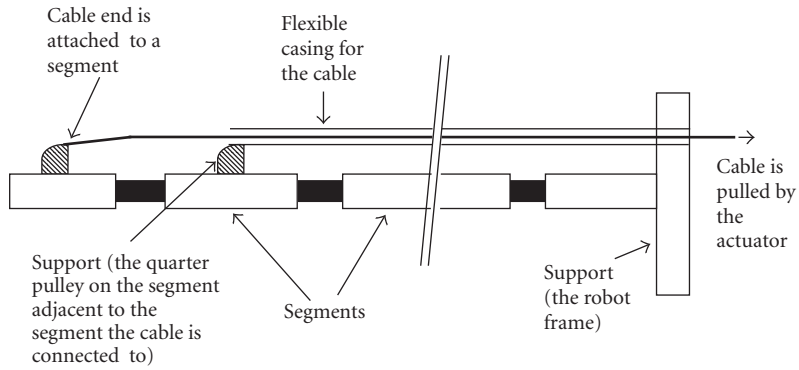

Figure 7: The detail of the cable design—one side only.

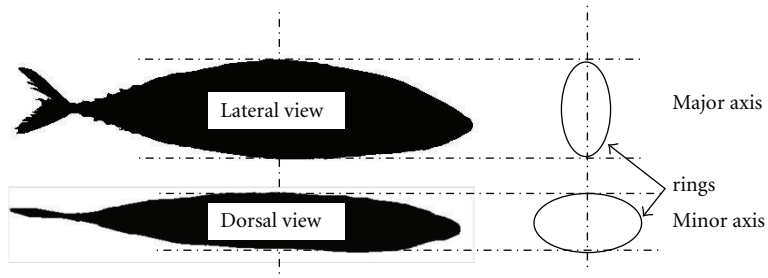

Figure 8: The dimension of the rings used for the haul.

(10) Figure 7 shows the detail of the nylon cable (C) design—it uses clutch cable design (as used in bicycles and cars). It is made up of flexible plastic other covering and nylon cable (inside).

9.3. Construction Process. A projected image of the life mackerel (Figure 8) is traced out on a wooden board, the major and minor axis dimension is taken at interval of 5 mm along the length of the traced model. The measurements at the widest part of the fish towards the frontal part are used for building ellipsoidal rings (Figure 9) (an approximation of the real shape of the life fish). These rings are then glued together to form the haul—Figure 10. The remaining half is cut into sections with 5 mm removed between adjacent segments and is replaced with rubber stripes (Figure 11) which act as the hinge (or revolute joint). The final assembly of the tail section is shown in Figure 12. Figure 13 is the lateral and dorsal view of the assembly. The nose cone is not yet attached to allow access into the haul. Furthermore, the servo motors were glued to the tail support in a serial fashion as shown in Figure 14. This arrangement is to allow the motors enter into the cavity of the haul (the front part) and to balance the weight of the robotic fish. Figure 15 shows a cut away view of how the servomotors are finally arranged inside the haul.

10. Tests on the Rubber Joint

The following tests were performed on the developed robotic joint; simulated loads, frequency softening effect of the rubber joints, and shape generation (biomimicry).

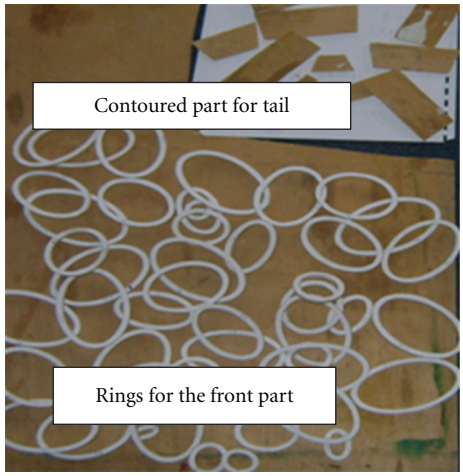

Figure 9: The tracing is translated into ring for the front part and contoured section for the rear part.

Figure 10: The rings were glued together to form the front part of the robot fish.

10.1. Test 1. For simulated loadings, the most critical portion of the model is the tail. Also,

(1) the peduncle (Figure 16) is the main propulsive organ for teleost species of fish (like mackerel) and is thus expected to experience the greatest load;

(2) it is required to bend at almost ±45° while in action;

(3) it has the thinnest portion of the whole body thus it is the "weakest link of a chain;"

(4) it has the highest angular velocity than the other tail sections.

A finite element analysis was used since rubber (a nonlinear) material is involved and the equations for solving its loading characteristics are constitutive equations. The tool selected is ANSYS Multiphysis version 10. The CAD environment was Autodesk Inventor 7. The raw data used for the wooden section is shown in Table 1.

Plywood is used for the support forming the segment and the fin.

Figure 11: The rubber is cut according to the shape of the tail—the first 2 stripes from the tail fin (left on this picture are 20 mm wide and the remaining ones are 25 mm wide).

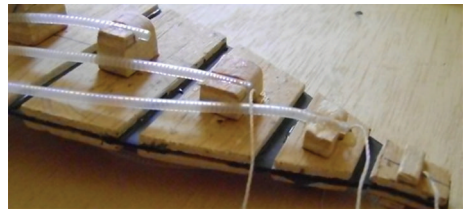

Figure 12: The assembled tail (joint) showing the polythene pipe through which the cables are treaded. The ends of the pipes are glued to the quarter pulley. The plywoods (1/8 in/3.175 mm) are glued to the rubber stripes to form the tail joints. The cables are connected to the next wooden support.

Lateral view

(a)

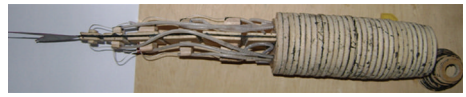

Dorsal view

(b)

Figure 13: The assembled fish robot.

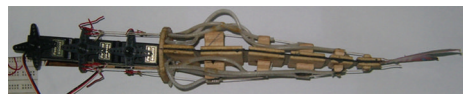

Figure 14: The three servomotors are attached with superglue (Cyanoacrylate glue) to themselves. Superglue was also used for the main bond between them and the wooden tail base with Araldite glue (Epoxy) acting as bulk support (being more voluminous).

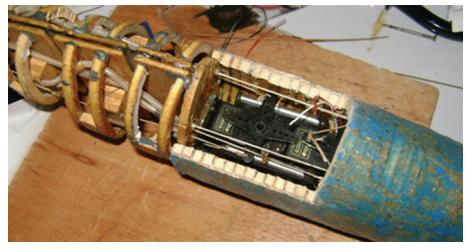

Figure 15: Cut view of the final arrangement.

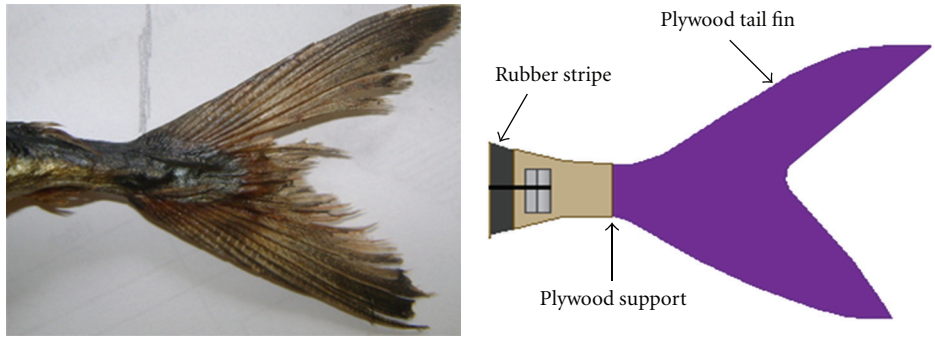

Figure 16: A fish peduncle.

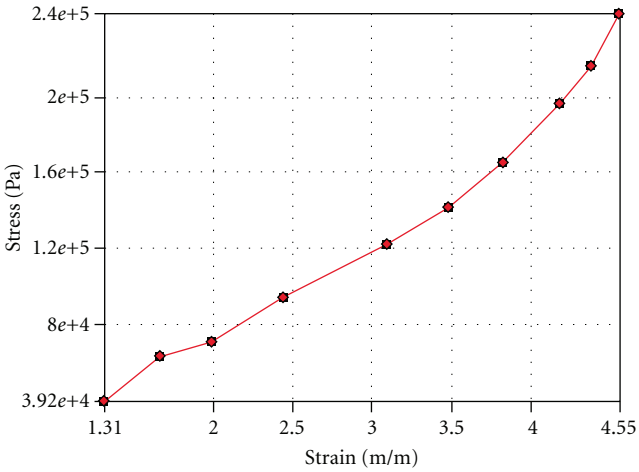

Figure 17: Uniaxial tensile test result on the sample rubber.

Table 1

Young modulus	5×10^9 Pa
Poisson's ratio	0.25
Density	500 kg/m^3
Tensile yield strength	1.5×10^7 Pa
Compressive yield strength	3.6×10^7 Pa
Tensile ultimate strength	3.1×10^7 Pa
Compressive ultimate strength	2.0×10^7 Pa

And for the rubber material, the data are uniaxial (Figure 17) and biaxial (Figure 18) test data.

The constitutive equation used was determined by using curve fitting tools provided in the ANSYS 10. The tool indicates that Mooney-Rivlin 5 parameter constutitive equation is adequate to predict the behaviour of the rubber sample as shown in Figure 19. The dotted line is the predicted, while the smoothline is the inputs (biaxial and uniaxial) as in Figures 17 and 18.

The following assumptions were also made in the simulation:

(1) the tail section is oscillating at max of 90° (±45°);

(2) it is oscillating at frequency of 1 Hz;

(3) it will operate in water with density of 990 kg/m^3 (sea water).

Figures 20 and 21 show how the loads were applied to the simulation model.

10.2. Test 2. Frequency-softening effect of the rubber joints commonly referred to as Payne effect is an effect whereby a rubber has reduced rigidity due to oscillations and is frequency dependent. A test was performed on the rubber material to know the critical frequency the joint should not exceed by subjecting a sample to oscillation at a fixed environmental temperature (especially). The amplitude of oscillation was 10 mm and the frequency varied from 0.5 Hz to 30 Hz. The softening effect was determined by measuring the lag in response of the support to square wave inputs operating at frequency of 0.5 Hz, 1 Hz, 5 Hz, 10 Hz, 15 Hz, 20 Hz, 25 Hz, and 30 Hz. The experimental setup is as shown in Figures 22 and 23. One computer generates precision signal that drives the motor that moves the rubber sample, the other one uses National instrument data logger to capture the motor movement (input), the time the motor reaches the peak displacement—detected by an optical sensor (output) and the environmental temperature using nickel—Constantan thermocouple junction. Figure 24 shows a sketch of the signal pattern when the test is being carried out.

10.3. Test 3. Shape generation (biomimicry). To test the performance of the model, a PIC18F4520 was programmed to generate pulse width modulated (PWM) signal to drive the three Futaba-3003 servomotors at 60° phase difference. Using Figure 5, one servomotor was attached to segment 1, the next one was attached to segment 2 and the last one was attached to the segment 4. Seven motion patterns were programmed into the microcontroller—dynamic turn left, dynamic turn right, sharp turn left, sharp turn right, tail oscillation amplitude up, tail oscillation amplitude down, tail oscillation speed up, tail oscillation speed down, and normal swim.

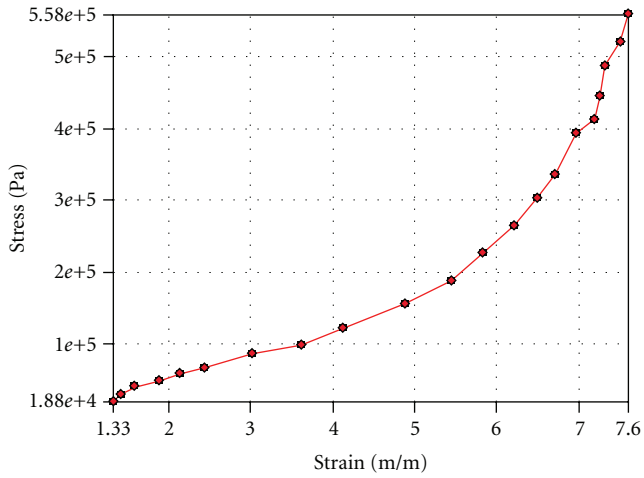

Figure 18: Biaxial tensile test result on the sample rubber.

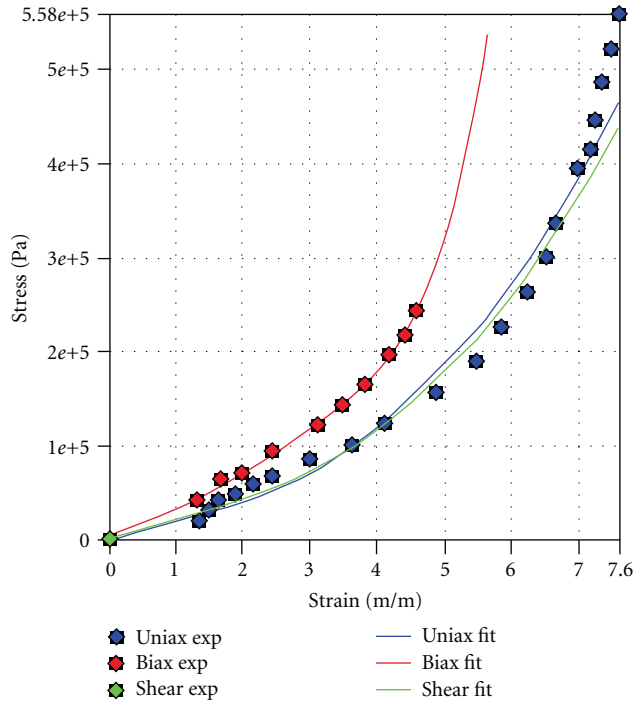

Figure 19: Mooney-Rivling 5 parameter constitutive equation used within the ANSYS 10 shows very close prediction of the rubber sample behavior. It means that Mooney-Rivling 5 parameter can be safely used for the Finite element analysis.

11. Results and Discussion of the Simulation on the Joint

Stress within the peduncle. Figure 25 shows the stress pattern after the simulation with the following results:

(1) von-Mises maximum stress (occurs on the fin) = 4.148×10^4 Pa = 41.5 kN/m^2;

(2) von-Mises minimum stress (multiple places) = 3.179×10 Pa = 0.03179 kN/m^2;

(3) von-Mises maximum stress in the rubber = 0.924×10^4 Pa = 9.24 kN/m^2.

The maximum stress any rubber joint will experience is 9.24 kN/m^2. The sample rubber used has been tested to be capable of handling stress up to 100 kN/m^2. Thus it will safely handle the loads in this weakest region.

The frequency softening effect was found to be critical at 25 Hz (see Figure 26) for this particular rubber sample, which means the oscillation should not exceed that value if serious softening is not to occur. Less lag value means that the rubber is getting soft. Figure 27 is the temperature variation at which the tests were carried out, stability of the environmental temperature is very critical to the accuracy of the result.

The shape generation result is as shown in Figure 28 which indicates a close pattern (biomimicry) to a life fish. "Skin" cover will smooth out sharp bends that may be present.

12. Experimental Verification of the Robotic Fish Performance

To assess the performance of the robotic fish, tests were performed in a stationary body of water at 20 cm depth (or 1.92 kPa pressure head). The water body is a shallow pond located at Ahmadu Bello University Faculty of Engineering. The pond has a depth range of 25 cm to 50 cm (equivalent pressure head of 2.4 kPa–4.9 kPa). The following tests were recorded using Sony Cyber-shot digital camera (model DSC-S730) at a resolution of 3 megapixels, F-stop of f/2.8, exposure time of 1/40 sec, ISO speed of 100:

(1) tail oscillation speed—this is the frequency at which the tail section moves from left to right and back again;

(2) dynamic turning (turning while swimming)—this is the turning performed while cruising. The robot tail oscillation is restricted to one side in this mode, see Figure 29;

(3) amplitude of oscillation of the tail—this is the amount of excursion the tail section makes from the middle line to either side;

(4) sharp turning—this is the turning procedure which involves bending like a coil or letter C and then uncoiling rapidly;

(5) swimming speed at different peduncle amplitude and different tail frequencies.

12.1. Results and Discussion of the Experiments. The following results were obtained. The maximum tail oscillation speed achieved is 1.7 Hz inside the pond. The speed is 4.3 Hz when not immersed inside the pond of water. This lowered speed is due to water drag.

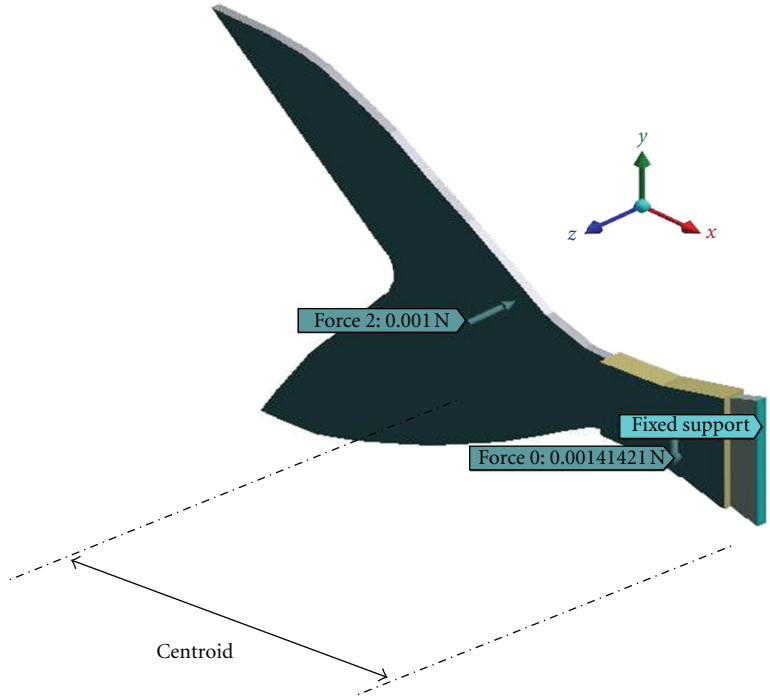

Figure 20: The simulation inputs: 0.001 N on the fin, 0.00141421 N (0.001 N—z-axis, 0.001 N—x-axis) on the plywood support.

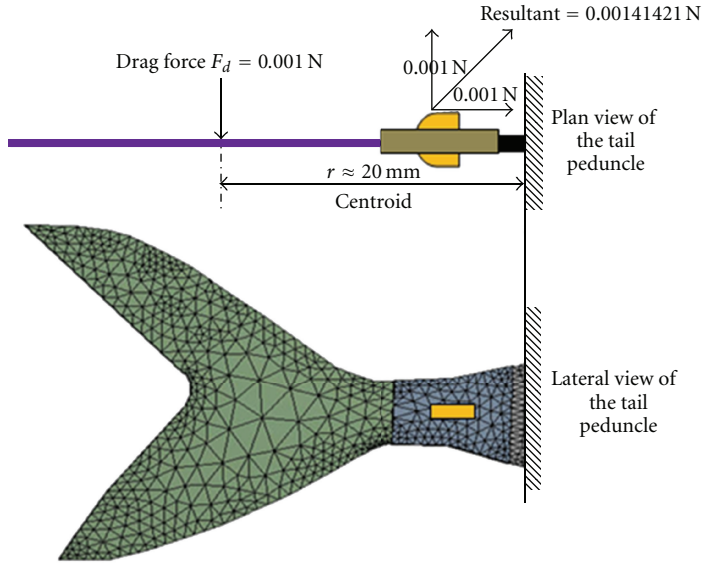

Figure 21: Simulated input loads—plan and side views. The finite element tool determines the centroid of the area.

During the dynamic turning test, the tail (at peduncle) was able to transits from 0° to 45°. Furthermore, the transition between normal swimming and dynamic turning for the whole tail section is noticeably smooth.

The amplitude of oscillation of the tail while swimming is tabulated as shown in Table 2. Three sections were used for measurement: the segment close to the base (the base is the portion joined to the haul), the segment at the very middle, and the segment to which the tail fin is attached to.

The ~90° maximum for the peduncle is an out of bound data resulting from the water pressure on it, that is, the peduncle was forced to bend that far while pushing the water away. The flexibility of rubber encourages this behavior.

For the sharp turning experimentation, the minimum turning radius achieved was 0.8 m which is approximately 2 times the robot fish body length of 0.394 m. The uncoiling delay was approximately 1 second. The programmed delay is fixed at 600 ms, the extra 400 ms lag is due to the motor inertia and the water environment and the rubber joints.

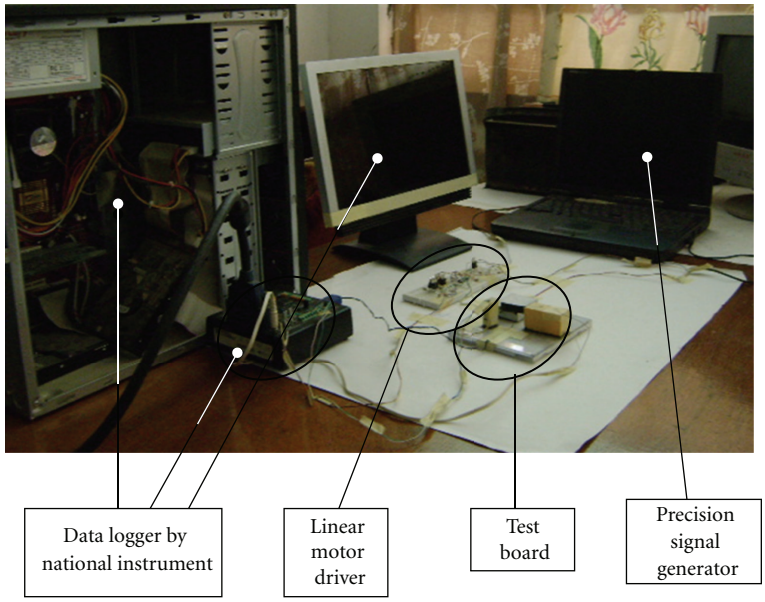

Figure 22: The frequency loss determination equipment.

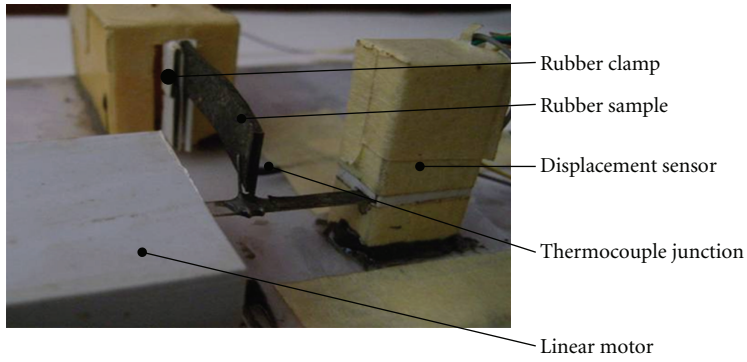

Figure 23: Closer view of the test board.

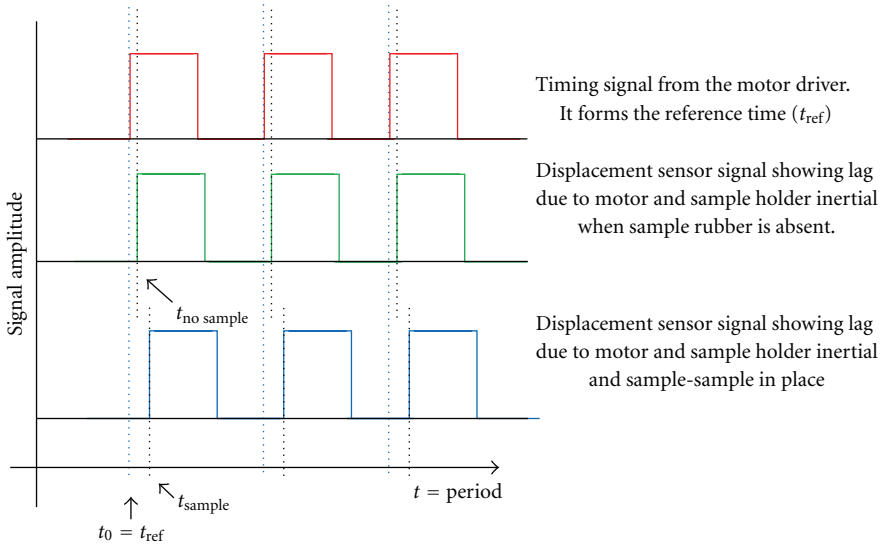

Figure 24: Signal pattern showing presence and absence of sample rubber. The delay is increased when sample is in place. The absolute value of this delay is obtained from $t_{sample} - t_{no\ sample} - t_{ref}$.

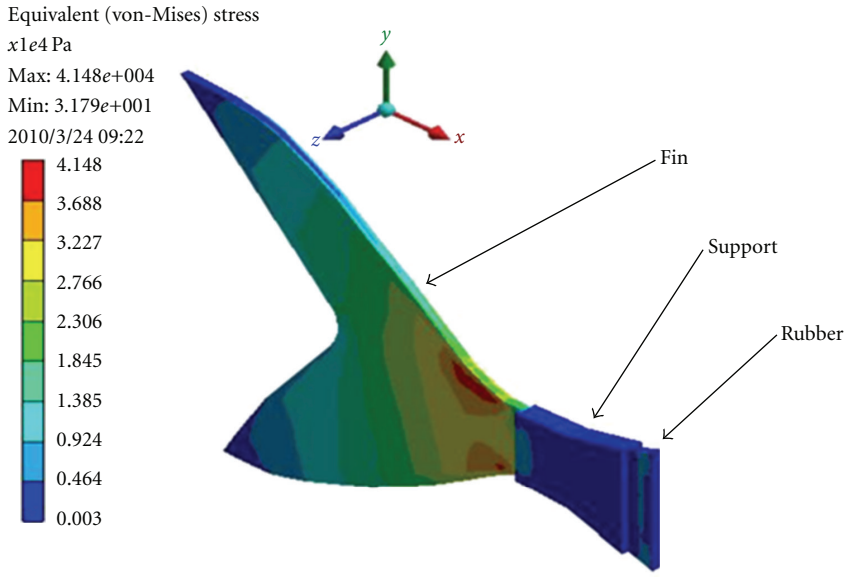

Figure 25: Simulation result—von-Mises stress acting within the peduncle using the simulated loads.

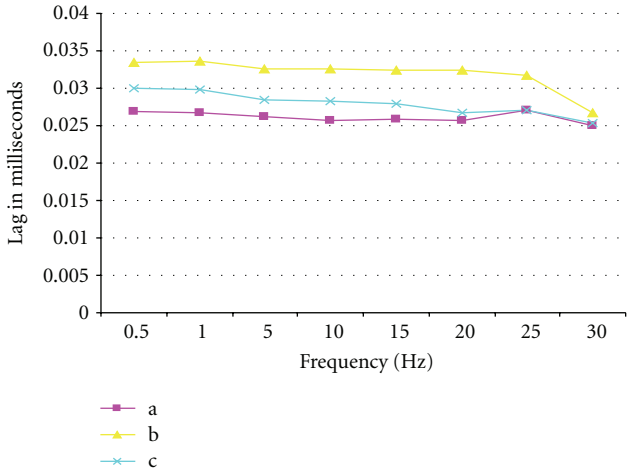

Figure 26: Progressive drops in response time with increasing frequency. The legend (a, b, c) refers to the environmental temperature as shown in Figure 27.

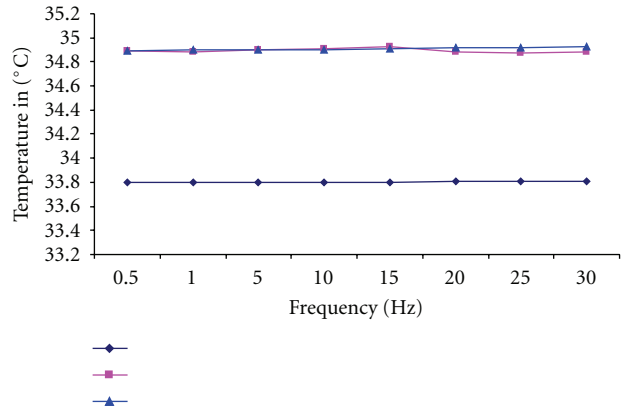

Figure 27: Ambient temperatures at which the tests were carried out.

The swimming speed at different peduncle amplitude and different tail frequencies is shown in Figure 30. In this paper, the measurement is focused on the peduncle amplitudes at oscillation frequencies of 0.5, 0.7, 0.9, 1.1, 1.3, 1.5, and 1.7 Hz. The result is comparable to that obtained by [60]. In this work and theirs, the speed of the fish robots increases with tail frequency. Also the increase amplitude leads to a relative increment in speed for each tail oscillation frequency. The relationship between tail frequency and speed is not linear.

The average maximum linear speed achieved was 0.985 m/s at the maximum tail oscillation (1.7 Hz) achieved inside the water pond. This is approximately 1/3 of that of a live mackerel which is 3.06 m/s (http://www.nmri.go.jp/eng/khirata/fish/general/speed/speede.htm). Compared to UPF-2001 robotic fish that has 0.97 m/s (http://www.nmri.go.jp//eng/khirata/fish) and the Essex G9 robotic fish [60] with linear speed of 0.2 m/s, the robot fish is faster at 0.985 m/s. This can be attributed to the tail design which used light material and thus allows faster tail beat (1.7 Hz inside water, 4.3 Hz in the air) than the Essex G9 fish that actually placed motors inside the tail which reduces its tail beat frequencies to 0.5 Hz. The UPF-2001 is also fast because it does not have motor in its tail, it uses lever to control its tail fin.

13. Conclusion

The design presented here (using rubber for the joint) has proved effective. The test carried out as indicated did not make it to collapse and, besides this, in comparison to other

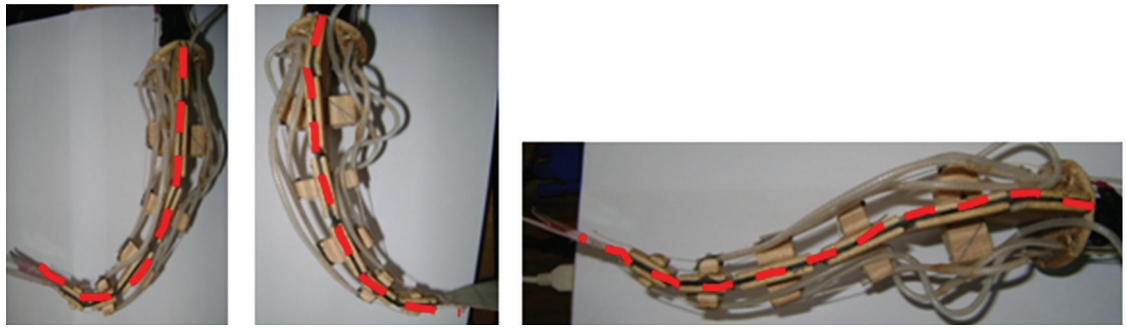

(a) (b) (c)

Figure 28: Static view of the tail bending left (a), bending right (b), and making a swimming shape (c).

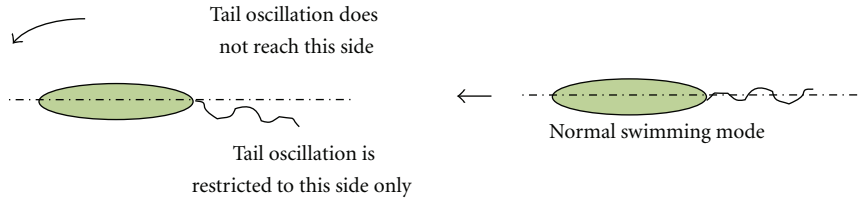

Figure 29: Dynamic turning while swimming.

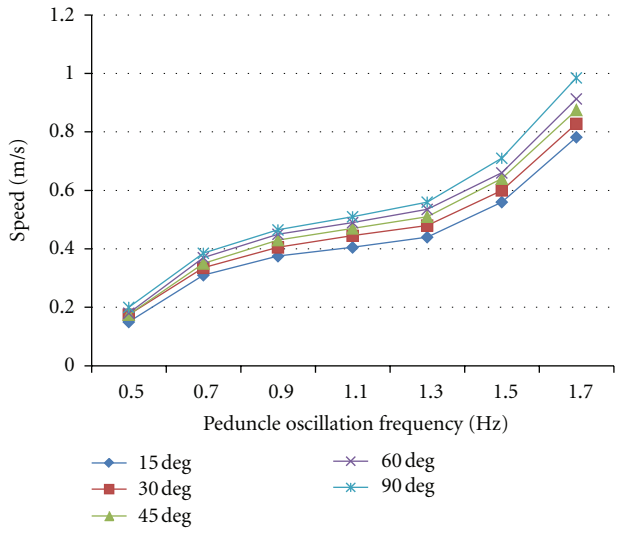

Figure 30: Speed of robot against peduncle (last segment) oscillation at different peduncle amplitude.

Table 2: The results of the amplitude variation of the tail sections.

Segment	Maximum	Minimum
1 (close to base)	~10° from center	~5° from center
2 (middle)	~45° from center	~10° from center
3 (attached to tail fin)	~90° from center	~45° from center

designs found in the literature (especially those reviewed) the tail design is obviously lighter and with less inertia because of the material used. Also this guarantee faster tail motion compared to the Essex G9 robotic fish robotic fish reviewed here.

Furthermore, the use of rubber implies long lasting joint with no need for lubrication or wear. If cost analysis were performed, the rubber material and wooden support (alternatively a plastic) should make it relatively cheap enough for mass production for distributive use or social robot working in corporation together say in a battle zone, exploration, search and rescue mission, and the like.

Acknowledgment

This project was supported by MacArthur Foundation and Ahmadu Bello University Board of Research grant.

References

[1] L. Peters, "Robotics," ERCIM News no. 42, July 2000, http://www.ercim.eu/.

[2] M. Jean-Arcady and G. Agnès, "Biologically inspired robots," in *Handbook of Robotics*, B. Siciliano and O. Khatib, Eds., pp. 1395–1418, Springer (Malestrom), 2008.

[3] J. C. Zufferey and D. Floreano, "Toward 30-gram autonomous indoor aircraft: vision-based obstacle avoidance and altitude control," in *Proceedings of the IEEE International Conference on Robotics and Automation*, pp. 2594–2599, April 2005.

[4] Harrison R. R. and Koch C, "A Silicon implementation of the fly's optomotor control system in letter by M.V. Srinivasan and Stephen DeWeerth," *Neural Computation*, vol. 12, pp. 2291–2304, Massachusetts institute of Technology, 2000.

[5] B. R. Fajen, W. H. Warren, S. Temizer, and L. P. Kaelbing, "A dynamical model of visually-guided steering, obstacle avoidance, and route selection," *International Journal of Computer Vision*, vol. 54, no. 1-3, pp. 13–34, 2003.

[6] M. V. Srinivasan, *Distance Perception in Insects*, Centre for Visual Sciences, Research School of Biological Sciences, Australian National University, Cambridge University Press, 1992.

[7] M. V. Srinivasan, S. W. Zhang, J. S. Chahl, G. Stange, and M. Garratt, "An overview of insect-inspired guidance for application in ground and airborne platforms," *Proceedings of the Institution of Mechanical Engineers, Part G*, vol. 218, no. 6, pp. 375–388, 2004.

[8] S. J. Park, M. B. Goodman, and B. L. Pruitt, "Analysis of nematode mechanics by piezoresistive displacement clamp," *Proceedings of the National Academy of Sciences of the United States of America*, vol. 104, no. 44, pp. 17376–17381, 2007.

[9] F. W. Grasso, "Flow- and chemo-sense for robot and lobster guidance in odor source tracking," in *Proceedings of the Neurotechnology for Biomimetic Robots Conference*, Nahant, Mass, USA, May, 2000.

[10] H. Yamada, S. Chigisaki, M. Mori, K. Takita, K. Ogami, and S. Hirose, "Development of amphibious snake-like robot ACMR5," in *Proceedings of the International Symposium on Robotics (ISR'05)*, p. 133, 2005.

[11] W. Cox, "Snake-like robot can crawl on land or swim," 2006, http://www.robotshop.com/gorobotics/the-news/latest-news/snake-like-robot-can-crawl-on-land-or-swim.

[12] K. J. Dowling, *Limbless locomotion: learning to crawl with a snake robot*, Ph.D. thesis, Robotics Institute Carnegie Mellon University, Pittsburg, Pa, USA, 1997.

[13] S. Ma and M. Watanabe, "Time-optimal control of kinematically redundant manipulators with limit heat characteristics of actuators," *Advanced Robotics*, vol. 16, no. 8, pp. 735–749, 2002.

[14] Microsoft Encarta Reference Library DVD, 2005.

[15] R. Brooks and A. M. Flynn, "Fast, cheap and out of control: robot invasion of the solar system," *Journal of the British Interplanetary Society*, vol. 42, no. 10, pp. 478–485, 1989.

[16] H. Matsuura, Y. Moriyama, S. Hirose, M. Mizutame, H. Shimada, and Y. Umetani, "Measuring/grinding system for water turbine runner," in *Proceedings of the 15th International Symposium on Industrial Robots*, pp. 199–206.

[17] M. Arai, Y. Tanaka, S. Hirose, H. Kuwahara, and S. Tsukui, "Development of 'Souryu-IV' and 'Souryu-V:' serially connected crawler vehicles for in-rubble searching operations," *Journal of Field Robotics*, vol. 25, no. 1-2, pp. 31–65, 2008.

[18] H. Choset and J. Y. Lee, "Sensor-based construction of a retract-like structure for a planar rod robot," *IEEE Transactions on Robotics and Automation*, vol. 17, no. 4, pp. 435–449, 2001.

[19] M. Yim, *Locomotion with a Unit Modular Reconfigurable Robot*, Department of Mechanical Engineering, Stanford University, Palo Alto, Calif, USA, 1994.

[20] C. Wilbur, W. Vorus, Y. Cao, and S. Currie, "A lamprey-based undulatory vehicle," in *Neurotechnology for Biomimetic Robots*, J. Ayers, J. Davis, and A. Rudolph, Eds., pp. 285–296, MIT Press, 2001.

[21] A. Crespi, A. Badertscher, A. Guignard, and A. J. Ijspeert, "AmphiBot I: an amphibious snake-like robot," *Robotics and Autonomous Systems*, vol. 50, no. 4, pp. 163–175, 2005.

[22] W. M. Kier and K. K. Smith, "Tongues, tentacles and trunks: the biomechanics of movement in muscular-hydrostats," *Zoological Journal of the Linnean Society*, vol. 83, no. 4, pp. 307–324, 1985.

[23] B. A. Skierczynski, R. J. A. Wilson, W. B. Kristan Jr., and R. Skalak, "A model of the hydrostatic skeleton of the leech," *Journal of Theoretical Biology*, vol. 181, no. 4, pp. 329–342, 1996.

[24] G. Robinson and J. B. C. Davies, "Continuum robots—a state of the art," in *Proceedings of the IEEE International Conference on Robotics and Automation, ICRA99*, pp. 2849–2854, May 1999.

[25] Y. Yekutieli, G. Sumbre, T. Flash, and B. Hochner, "How to move with no rigid skeleton?" *Biologist*, vol. 49, no. 6, pp. 250–254, 2002.

[26] Y. Yekutieli, R. Sagiv-Zohar, B. Hochner, and T. Flash, "Dynamic model of the octopus arm. II. Control of reaching movements," *Journal of Neurophysiology*, vol. 94, no. 2, pp. 1459–1468, 2005.

[27] Y. Yekutieli, R. Sagiv-Zohar, R. Aharonov, Y. Engel, B. Hochner, and T. Flash, "Dynamic model of the octopus arm. I. Biomechanics of the octopus reaching movement," *Journal of Neurophysiology*, vol. 94, no. 2, pp. 1443–1458, 2005.

[28] G. S. Chirikjian and J. W. Burdick, "Kinematics of hyper-redundant robot locomotion with applications to grasping," in *Proceedings of the IEEE International Conference on Robotics and Automation*, pp. 720–725, April 1991.

[29] M. Gavin, 2010, http://www.snakerobots.com/.

[30] S. Hirose and A. Morishima, "Design and control of a mobile robot with an articulated body," *International Journal of Robotics Research*, vol. 9, no. 2, pp. 99–113, 1990.

[31] K. Osuka and H. Kitajima, "Development of Mobile Inspection Robot for Rescue Activities: MOIRA," in *Proceedings of the IEEE/RSJ International Conference on Intelligent Robots and Systems*, pp. 3373–3377, October 2003.

[32] G. Grzegorz, M. G. Hansen, and B. Johann, "The OmniTread serpentine robot for industrial inspection and surveillance," *International Journal on Industrial Robots*, vol. IR32-2, pp. 139–148, 2005.

[33] B. A. Trimmer, A. E. Takesian, B. M. Sweet, C. B. Rogers, D. C. Hake, and D. J. Rogers, "Caterpillar locomotion and burrowing robots," in *Proceedings of the 7th International Symposium on Technology and Mine Problem*, Monterey, Calif, USA, 2006.

[34] E. Shammas, A. Wolf, H. B. Brown Jr., and H. Choset, "New joint design for three-dimensional hyper redundant robots," in *Proceedings of the IEEE International onference on Robotics and Automation*, Las Vegas, Nev, USA, October 2003.

[35] Y. Hiroya and H. Shigeo, "Development of practical 3-dimentinal active cord mechanism ACM-R4," *Journal of Robotics and Mechatronics*, vol. 18, no. 3, pp. 305–311, 2006.

[36] M. Makoto and H. Shigeo, "Locomotion of 3D snake-like robots; shifting and rolling control of active cord mechanism ACM-R3," *Journal of Robotics and Mechatronics*, vol. 18, no. 5, pp. 521–528, 2006.

[37] K. Bonsor, "How snakebots work," 2003, http://electronics.howstuffworks.com/snakebot.htm.

[38] E. Shammas, W. Alon, B. H.Ben Jr., and C. Howie, "New joint design for three-dimensional hyper redundant robots," in *Proceedings of the IEEE International Conference on Robotics and Automation*, Las Vegas, Nev, USA, October 2003.

[39] A. Wolf, H. B. Brown, R. Casciola et al., "A mobile hyper redundant mechanism for search and rescue tasks," in *Proceedings of the IEEE/RSJ International Conference on Intelligent Robots and Systems*, Las Vegas, Nev, USA, October 2003.

[40] M. J. Farabee, "Muscular and skeletal systems," 2001, http://www.emc.maricopa.edu/faculty/farabee/BIOBK/BioBook-MUSSKEL.html.

[41] D. A. Kelly, "Penises as variable-volume hydrostatic skeletons," *Annals of the New York Academy of Sciences*, vol. 1101, pp. 453–463, 2007.

[42] C. Alscher and W. J. Beyn, "Simulating the motion of the leech: a biomechanical application of DAEs," *Numerical Algorithms*, vol. 19, no. 1-4, pp. 1–12, 1998.

[43] W. A. Woods Jr., S. J. Fusillo, and B. A. Trimmer, "Dynamic properties of a locomotory muscle of the tobacco hornworm Manduca sexta during strain cycling and simulated natural crawling," *Journal of Experimental Biology*, vol. 211, no. 6, pp. 873–882, 2008.

[44] A. Dorfmann, B. A. Trimmer, and W. A. Woods, "A constitutive model for muscle properties in a soft-bodied arthropod," *Journal of the Royal Society Interface*, vol. 4, no. 13, pp. 257–269, 2007.

[45] J. D. Humphrey, "Continuum biomechanics of soft biological tissues," *Proceedings of the Royal Society A*, vol. 459, no. 2029, pp. 3–46, 2003.

[46] R. W. Ogden and D. G. Roxburgh, "A pseudo-elastic model for the Mullins effect in filled rubber," *Proceedings of the Royal Society A*, vol. 455, no. 1988, pp. 2861–2877, 1999.

[47] K. L. Paap, M. Dehlwisch, and B. Klaassen, "GMD-Snake: a semi-autonomous snake-like robot," in *Proceedings of the 3rd International Symposium on Distributed Autonomous Robot Systems (DARS'96*, RIKEN, Saitama, Japan, October, 1996.

[48] A. Wolf, H. H. Choset, H. B. Brown, and R. W. Casciola, "Design and control of a mobile hyper-redundant urban search and rescue robot," *Advanced Robotics*, vol. 19, no. 3, pp. 221–248, 2005.

[49] O. Adria, H. Streich, and J. Hertzberg, "Dynamic replanning in uncertain environmentsfor a sewer inspection robot," *Inernational Journal of Advanced Robotic Systems*, vol. 1, no. 1, pp. 33–38, 2004.

[50] http://www.ornl.gov/info/ornlreview/rev26-34/text/tramain.html.

[51] Y. Mark, 2010, http://robotics.stanford.edu/users/mark/bio.html.

[52] H. Matsuura, M. Mizutame, Y. Moriyama, H. Shimada, S. Hirose, and Y. Umetani, "Measuring/grinding system for water turbine runner," in *Proceedings of the 15th International Symposium on Industrial Robots*, pp. 199–206, Tokyo, Japan, 1985.

[53] J. Borenstein, M. Hansen, and H. Nguyen, "The OmniTread OT-4 serpentine robot for emergencies and hazardous environments," in *Proceedings of the 1st Joint Emergency Preparedness and Response/Robotic and Remote Systems Topical Meeting*, pp. 239–246, February 2006.

[54] K. Streitlien, G. S. Triantafyllou, and M. S. Triantafyllou, "Efficient foil propulsion through vortex control," *AIAA Journal*, vol. 34, no. 11, pp. 2315–2319, 1996.

[55] Anderson J. M., *Vorticity control for efficient propulsion*, Ph.D. dissertation, Massachusetts Institute of Technology, Woods Hole, Oceanographic Institution Joint Program, Woods Hole, Mass, USA, 1996.

[56] S. Guo, T. Fukuda, N. Kato, and K. Oguro, "Development of underwater microrobot using ICPF actuator," in *Proceedings of the 1998 IEEE International Conference on Robotics and Automation. Part 1 (of 4)*, pp. 1829–1834, May 1998.

[57] N. Kato, "Control performance in the horizontal plane of a fish robot with mechanical pectoral fins," *IEEE Journal of Oceanic Engineering*, vol. 25, no. 1, pp. 121–129, 2000.

[58] J. H. Liang, T. M. Wang, H. X. Wei, and W. Tao, "Research and development of underwater robofish II- development of a small experimental robofish," *Robot*, vol. 24, no. 3, pp. 234–238, 2002.

[59] Y. U. Jun-zhi, C. Er-kui, W. Shuo, and T. A. N. Min, "Research evolution and analysis of biomimetic robot fish," *Journal of Control Theory and Applications*, vol. 20, no. 4, pp. 485–491, 2003.

[60] J. Liu and H. Hu, "Building a 3D simulator for autonomous navigation of robotic fishes," in *Proceedings of the IEEE/RSJ International Conference on Intelligent Robots and Systems*, Sendai, Japan, Semptember, 2004.

[61] J. Liu and H. Hu, "Building a simulation environment for optimising control parameters of an autonomous robotic fish," in *Proceedings of the 9th Chinese Automation & Computing Society Conference in the UK*, Luton, UK, September 2003.

[62] D. Barrett, 1994, http://web.mit.edu/towtank/www/Tuna/tuna.html.

[63] K. J. Muir, 1996, http://web.mit.edu/towtank/www/Pike/pike.html.

[64] http://www.nmri.go.jp/eng/khirata/fish.